

# Closing the sea surface mixed layer temperature budget from in-situ observations alone: Operation Advection during BoBBLE

V. Vijith<sup>1,2</sup>, P. N. Vinayachandran<sup>1,\*</sup>, Benjamin G. M. Webber<sup>3</sup>, Adrian J. Matthews<sup>4</sup>, Jenson V. George<sup>1</sup>, Vijay Kumar Kannaujia<sup>5</sup>, Aneesh A. Lotliker<sup>6</sup>, and P. Amol<sup>7</sup>

<sup>1</sup>Centre for Atmospheric and Oceanic Sciences, Indian Institute of Science, Bangalore, India

<sup>2</sup>School of Marine Sciences, Cochin University of Science and Technology, Kochi, India (present affiliation)

<sup>3</sup>Climatic Research Unit, School of Environmental Sciences, Centre for Ocean and Atmospheric Sciences, University of East Anglia, UK

<sup>4</sup>School of Environmental Sciences and School of Mathematics, Centre for Ocean and Atmospheric Sciences, University of East Anglia, UK

<sup>5</sup>CSIR-National Institute of Oceanography, Goa, India

<sup>6</sup>Indian National Centre for Ocean Information Services, Hyderabad, India

<sup>7</sup>CSIR-National Institute of Oceanography, Regional Center, Visakhapatnam, India

\*vinay@iisc.ac.in

## ABSTRACT

This document includes supplementary figures.

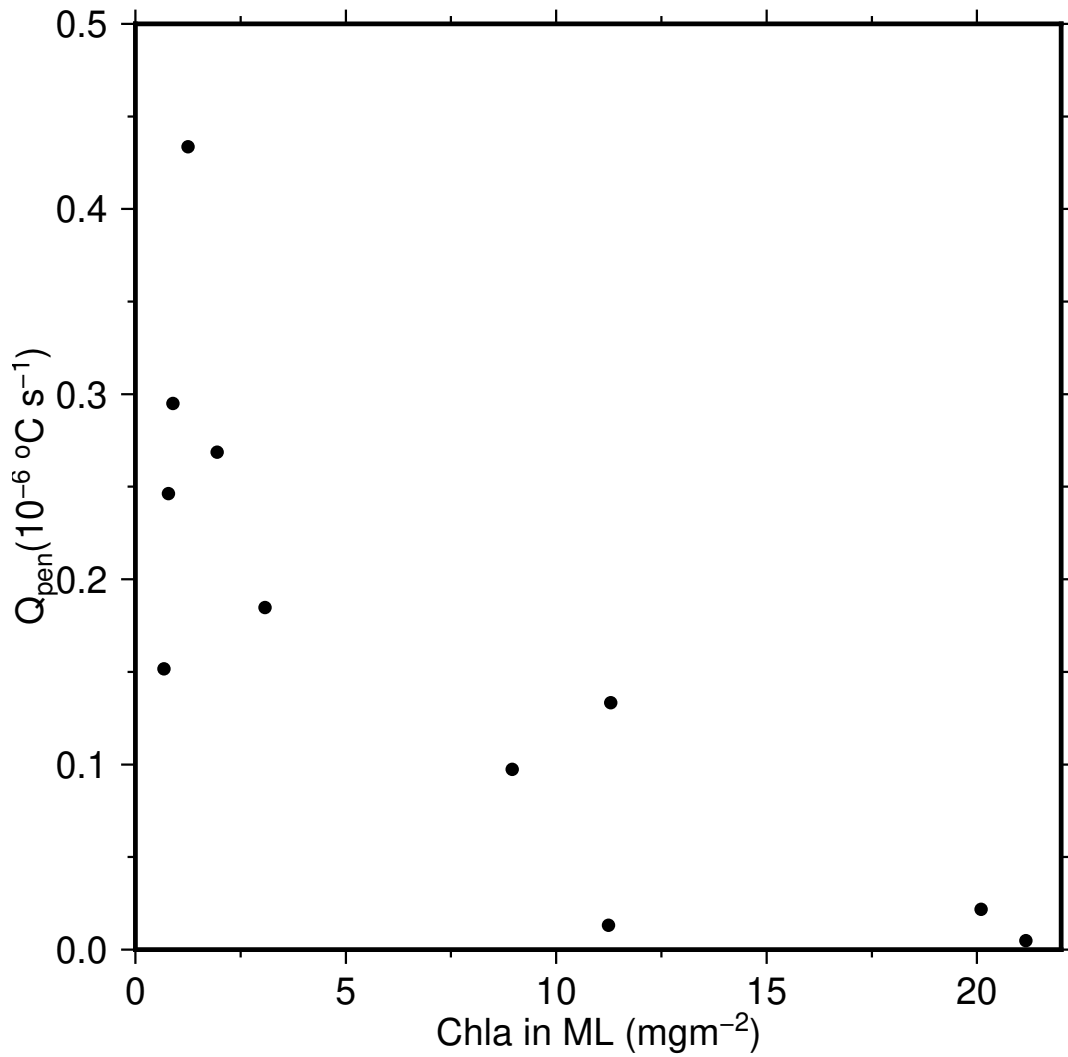


**Figure S1.** Daily averaged penetrative short-wave radiation at the base of the ML as a function of total chlorophyll in the ML.

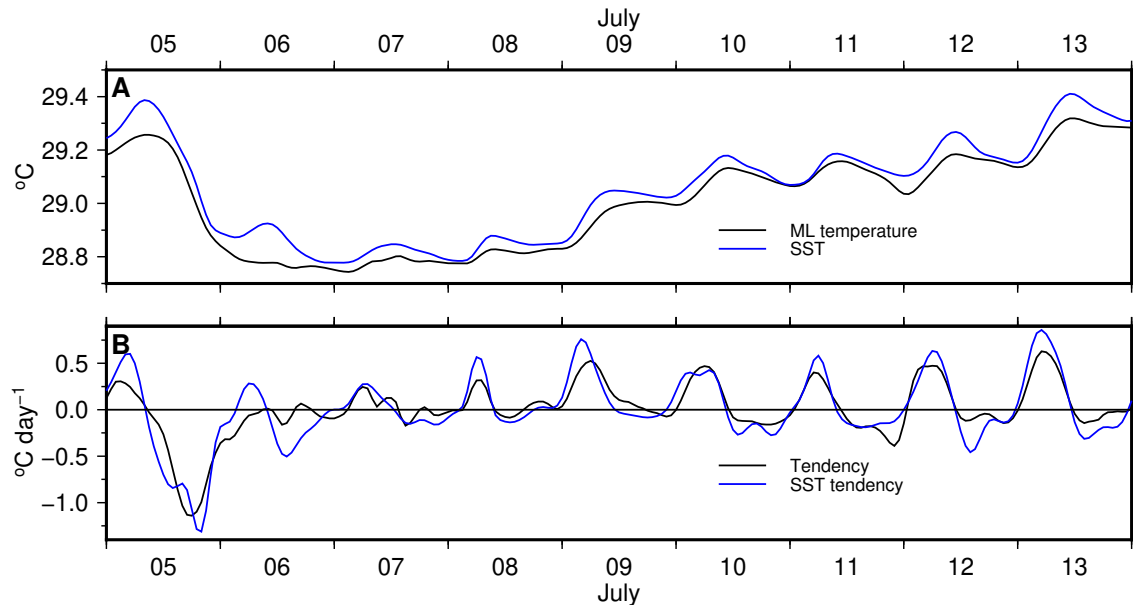


**Figure S2.** Time series of ML-averaged temperature and SST, (B) tendencies of the ML-averaged temperature and SST. All the variables are smoothed using a 4-hour moving window to remove high-frequency noise.

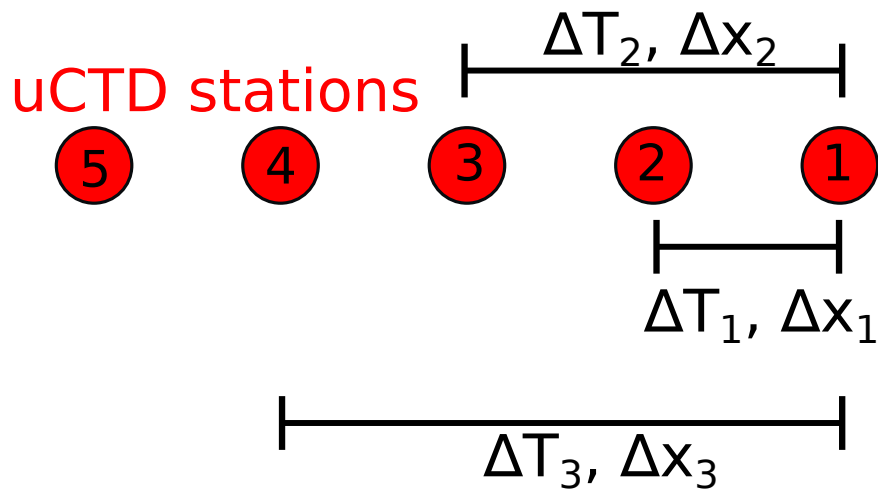


**Figure S3.** Schematic diagram illustrating the gradient calculation using the uCTD section.  $\Delta T_i$  denote the difference of mixed-layer averaged temperature at each uCTD station with the temperature at the first uCTD station.  $\Delta x_i$  denote the distance between each uCTD station from the first station. Suffix,  $i=1,5$ , denote the uCTD station number.

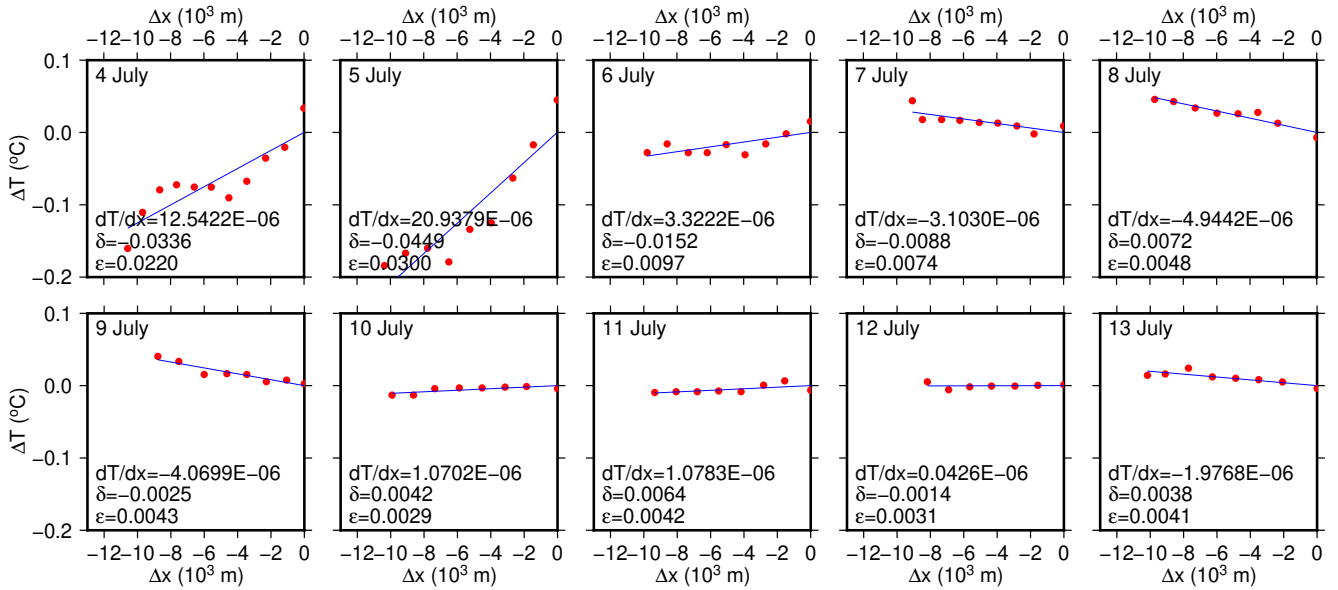


**Figure S4.**  $\Delta T$  plotted as a function of  $\Delta x$  for each day of measurement using the westward leg of the uCTD. The method of computation of the differences is shown in Fig. S3. The slope of the straight-line fit is the gradient in the zonal direction ( $\frac{\partial T}{\partial x}$ ),  $\delta$  is the offset and  $\epsilon$  is the root mean square value of the random variability. Note that  $\delta$  is removed from each of these fits.

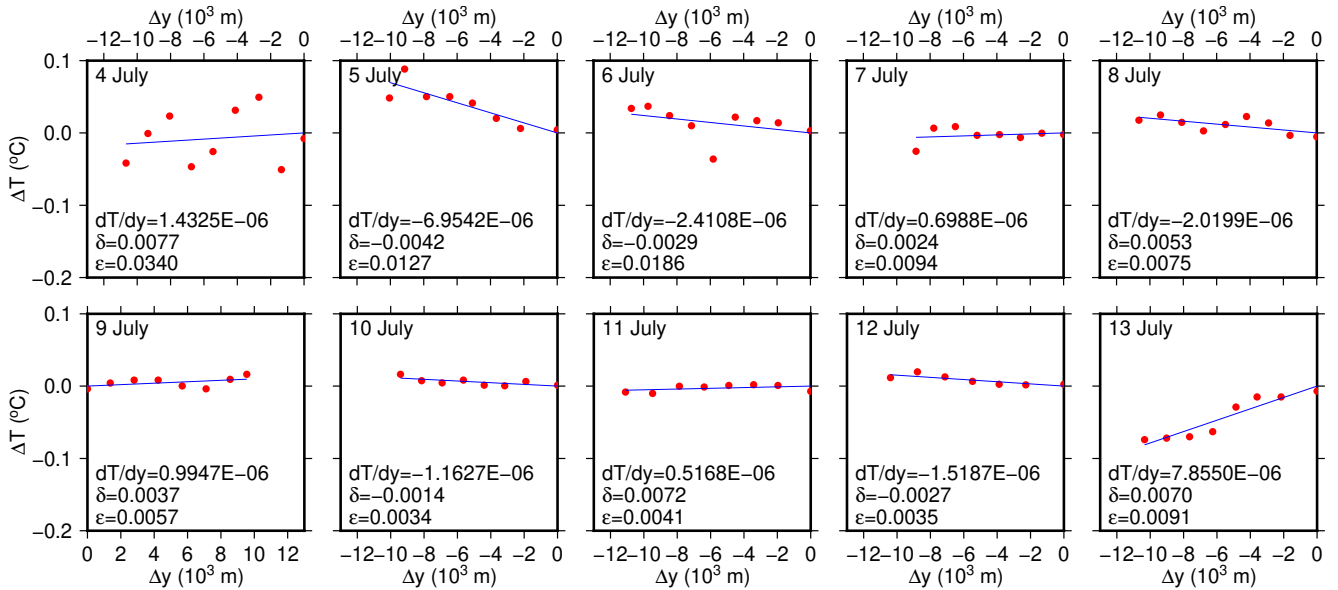


**Figure S5.** Same as Fig. S4. But using the southward leg of the uCTD for estimating the meridional gradient of temperature ( $\frac{\partial T}{\partial y}$ ).

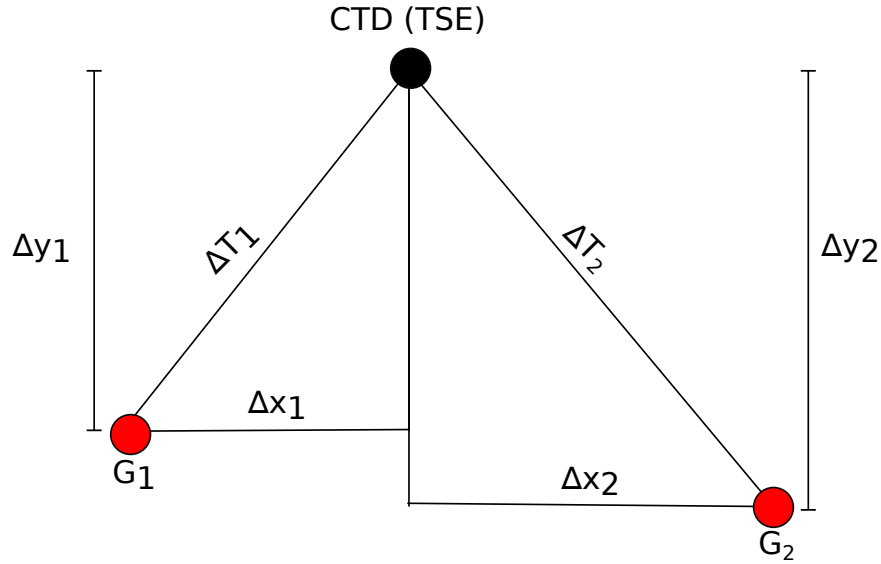


**Figure S6.** Schematic diagram illustrating the gradient calculation based on the ship-glider triangular configuration.  $\Delta T_i$  denote the difference of mixed-layer averaged temperature at each glider station with the temperature at TSE measured using CTD.  $\Delta x_i$  and  $\Delta y_i$  denote the zonal and meridional distance, respectively, between each glider from TSE.

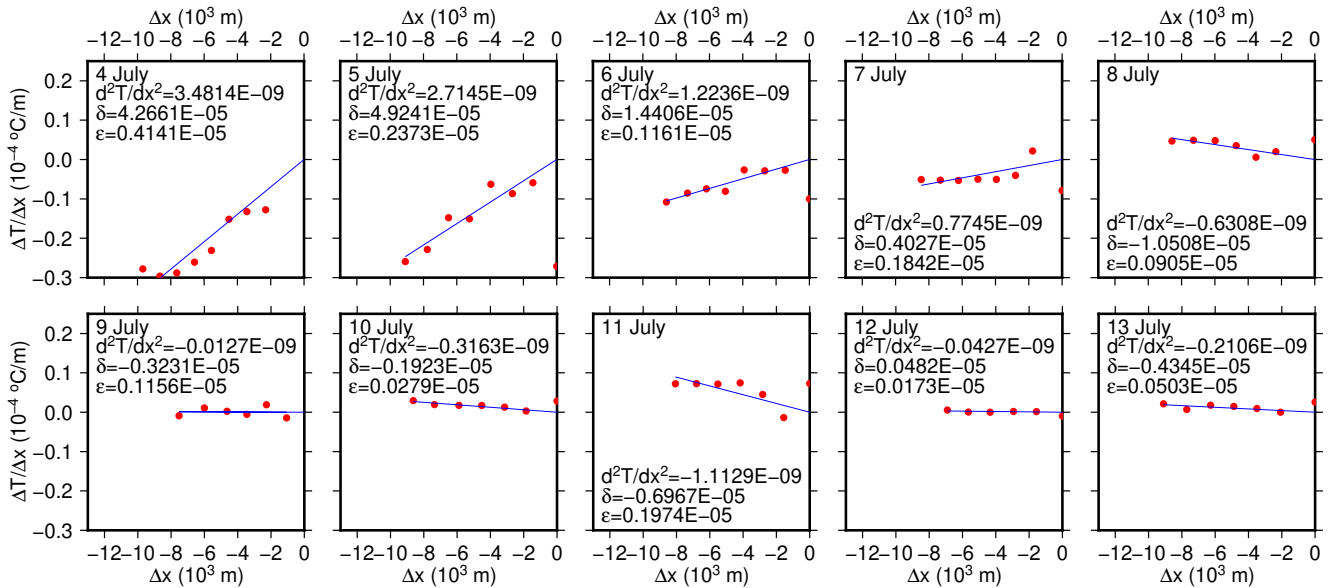


**Figure S7.**  $\Delta T/\Delta x$  differences plotted as a function of  $\Delta x$  for each day of measurement using the westward leg of the uCTD. The slope of the straight-line fit is the second derivative of temperature in the zonal direction ( $\frac{\partial^2 T}{\partial x^2}$ ),  $\delta$  is the offset and  $\epsilon$  is the root mean square of the random variability. Note that  $\delta$  is removed from each of these fits.

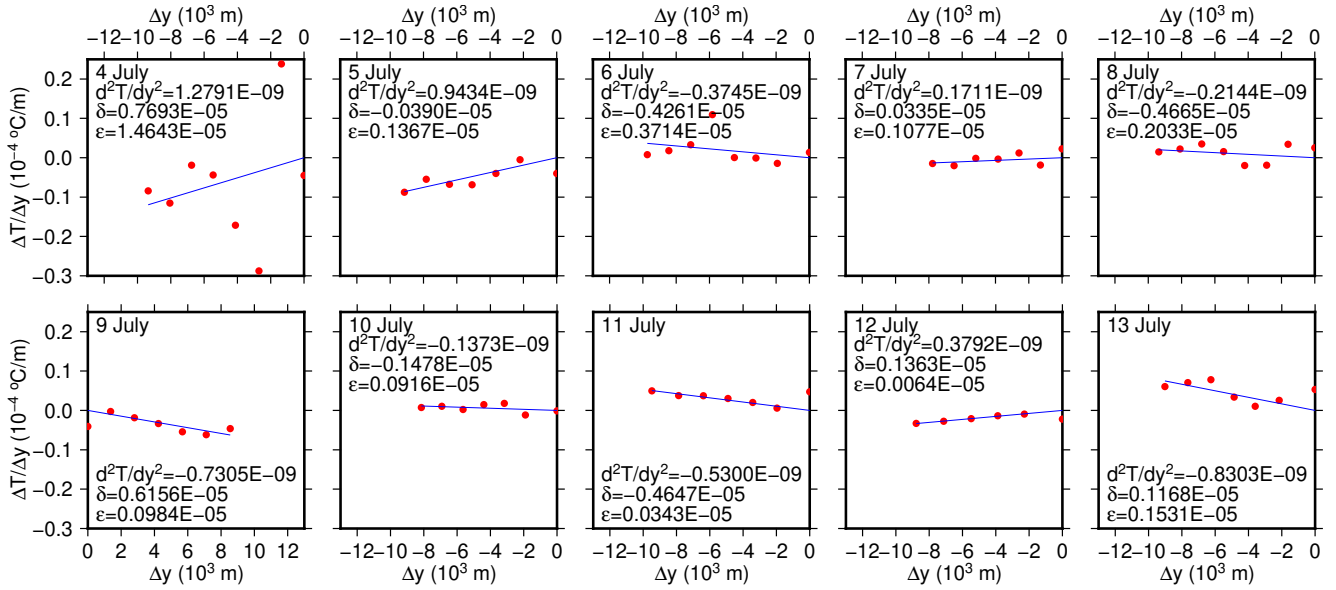


**Figure S8.** Same as Fig. S7. But using the southward leg of the uCTD for estimating the second derivative of temperature in the zonal direction ( $\frac{\partial^2 T}{\partial y^2}$ ).

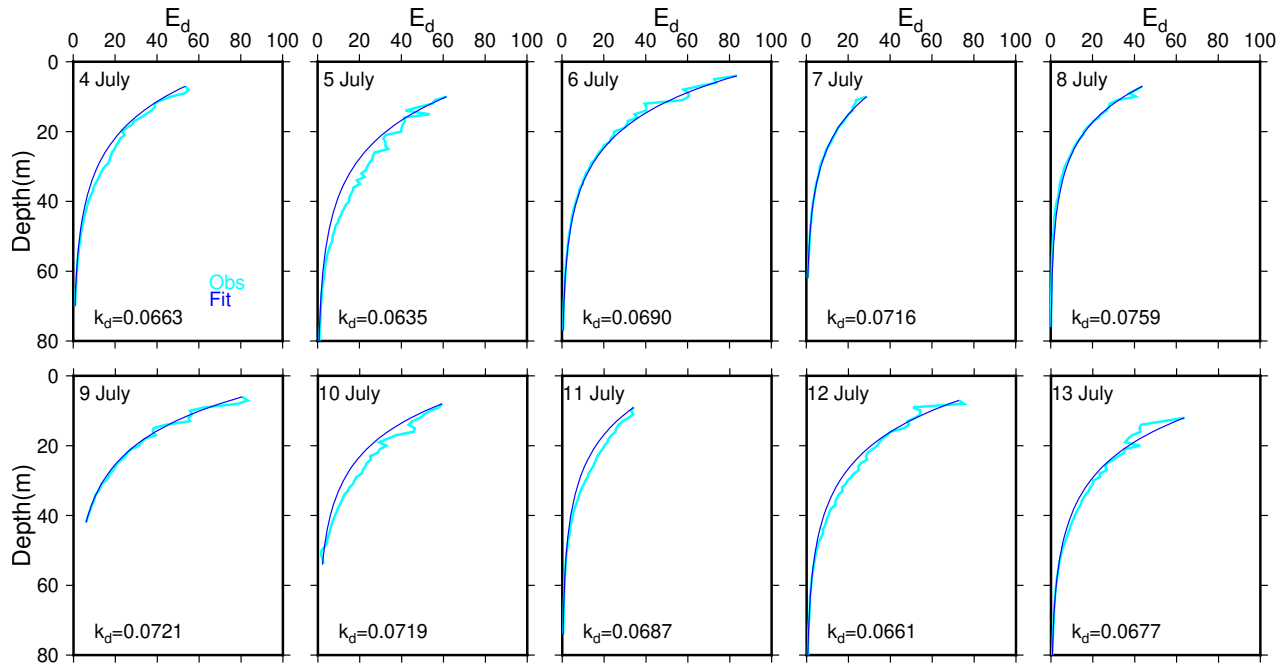


**Figure S9.** Comparison of downwelling irradiance averaged over the visible spectrum (400–700 nm) measured during the time-series observation at TSE with an exponential fit based on an averaged  $k_{PAR}$  equal to 0.0682.